Aerosol and Air Quality Research

ORIGINAL RESEARCH
https://doi.org/10.4209/aaqr.210376

Learnings from COVID-19 Forced Lockdown on Regional Air Quality and Mitigation Potential for South Asia

Special Issue:
Special Issue on Air Pollution and its Impact in South and Southeast Asia (I)

Abhishek Upadhyay[1], Parth Sarathi Mahapatra[1], Praveen Kumar Singh[1,2], Sishir Dahal[1], Suresh Pokhrel[1], Amit Bhujel[1], Indu Bikram Joshi[3], Shankar Prasad Paudel[3], Siva Praveen Puppala[1*†], Bhupesh Adhikary[1*†]

[1] International Centre for Integrated Mountain Development (ICIMOD), G.P.O. Box 3226, Kathmandu, Nepal
[2] Centre of Excellence in Disaster Mitigation and Management, Indian Institute of Technology Roorkee, Roorkee, Uttarakhand-247667, India
[3] Department of Environment, Ministry of Forests and Environment, Kathmandu, Nepal

ABSTRACT

South Asia is a hotspot of air pollution with limited resilience and hence, understanding the mitigation potential of different sources is critically important. In this context the country lockdown initiated to combat the COVID-19 pandemic (during March and April 2020 that is the pre-monsoon season) provides an unique opportunity for studying the relative impacts of different emission sources in the region. Here, we analyze changes in levels of air quality species across the region during selected lockdown periods using satellite and in-situ datasets. This analysis compares air quality levels during the lockdown against pre-lockdown conditions as well as against regional long-term mean. Satellite derived AOD, NO_2, and CO data indicates an increase of 9.5%, 2%, and 2.6%, respectively, during the 2020 lockdown period compared to pre-lockdown over the South Asia domain. However, individual country statistics, urban site data, and industrial grid analysis within the region indicate a more varied picture. Cities with high traffic loads reported a reduction of 12–39% in columnar NO_2 during lockdown, in-situ $PM_{2.5}$ measurements indicate a 23–56% percent reduction over the country capitals and columnar SO_2 has an approximate reduction of 50% over industrial areas. In contrast, pollutant emissions from natural sources e.g., from biomass burning were observed to be adversely affecting the air quality in this period potentially masking expected lockdown related air quality improvements. This study demonstrates the need for a more nuanced and situation specific understanding of sources of air pollutants (anthropogenic and natural) and for these sources to be better understood from the local to the regional scale. Without this deeper understanding, mitigation strategies cannot be effectively targeted, wasting limited resources as well as risking unintended consequences both for the atmosphere and how mitigation action is perceived by the wider public.

Keywords: COVID-19, Regional air quality, Forest fire, Satellite data, Mitigation

OPEN ACCESS

Received: December 9, 2021
Revised: February 2, 2022
Accepted: March 12, 2022

*** Corresponding Authors:**
Siva Praveen Puppala
sivapraveen.puppala@icimod.org
Bhupesh Adhikary
bhupesh.adhikary@icimod.org

† These authors contributed equally to this work

Publisher:
Taiwan Association for Aerosol Research
ISSN: 1680-8584 print
ISSN: 2071-1409 online

Copyright: The Author(s). This is an open access article distributed under the terms of the Creative Commons Attribution License (CC BY 4.0), which permits unrestricted use, distribution, and reproduction in any medium, provided the original author and source are cited.

1 INTRODUCTION

The effects of the coronavirus disease (COVID-19) global pandemic are wide ranging and of high impact. According to the World Health Organization (WHO), the first reported case was in December 2019 in the Wuhan district, Hubei Province, China (Li *et al.*, 2020; WHO Newsroom, 2020). The rapidity of its transmission globally and severity of its impacts lead to a global public health emergency (Lai *et al.*, 2020; Phua *et al.*, 2020). Mortality and morbidity rates rapidly rose and public health concerns lead to the conditions of "lockdowns" where movement of people and economic activity was highly restricted to reduce the spread of the disease. Lockdown

related restrictions on industry and transport affected global and regional economies (ICIMOD, 2020; World Bank, 2020). Another result of these lockdowns were reports of reductions in air, water, and noise pollution levels, reduced waste generation and increased atmospheric visibility (McNeill, 2020; Zambrano-Monserrate *et al.*, 2020).

Air pollution or air quality (AQ) is a pressing environmental issue with 91% of world population living with air pollution levels above WHO air quality guideline thresholds (WHO, 2022). AQ received increased public attention during the pandemic times in many parts of the world due to media reporting of anecdotal evidence suggesting a general improvement in highly polluted regions. A number of studies have indeed reported decrease in primary pollutants ($PM_{2.5}$, CO, NO_x) at a number of locations as well as in some cases increases in secondary pollutants such as ozone (O_3). Rates and levels of decrease have been shown to be variable globally depending on species and location (Fattorini and Regoli, 2020; Sharma *et al.*, 2020b; Venter *et al.*, 2020). These reported changes were shown to be negligible or did not follow a fixed trend on regional scales (Kanniah *et al.*, 2020; Menut *et al.*, 2020). This is taken to indicate that regional-scale studies were needed to better understand the impacts on AQ of COVID-19 restrictions and changes. South Asia (SA) is a global air pollution hotspot, that contains approximately 25% of the global population (United Nations, 2019) and a wide range of areas with sensitive biodiversity and fragile ecosystem (Wester *et al.*, 2019). Regional lockdowns and restrictions have provided an unprecedented opportunity to study AQ due to the enforced reduction in human movement and industrial activity in the SA region. This is particularly important in SA as the region is impacted by a wide variety of emission sources both anthropogenic and natural. Anthropogenic sources include crop residue burning, household cooking and heating, waste burning, emission from transportation, industrial activity and coal-based power generation, etc. (e.g., Jayarathne *et al.*, 2017; Saikawa *et al.*, 2019). Regional natural sources of emissions include forest fires, recirculation of mineral dust, seas salts and natural emissions (Jena *et al.*, 2015; Vadrevu *et al.*, 2019). This non-homogeneous restriction on air polluting sectors presents an opportunity to understand sector-specific contribution of different emission sources to AQ in the region at a range of scales from region to country to city. The economic impact of restricted activity did not affect all sectors equally with intensive sectors such as transport being affected more than residential sector. The lockdown resulted in a reduction of 10–31% in GDP, the equivalent of approximately 307–921 billion dollars (Kanitkar, 2020) primarily associated with restrictions on the transport, industry, and power sectors. Thus, providing an opportunity to understand the potential of implementing mitigation measures in these sectors and its associated costs. In this manuscript, we examine the heterogeneous impacts of lockdown on AQ drivers over SA using satellite and in-situ datasets to better understand future scenarios for mitigation of poor AQ. This study also highlights the need for a sector and or activity based understanding of AQ to enable effective and efficient implementation of mitigation strategies, especially in regions with potentially limited infrastructure and resource.

2 MATERIALS AND METHOD

In this study, we quantify the impact of COVID-19 and associated restriction on levels of aerosol and gaseous pollutants over the selected SA domain using satellite and in-situ data. The focus countries were Afghanistan, Bangladesh, Bhutan, India, Myanmar, Nepal and Pakistan with a deeper analysis of Nepal as an example of changes observed in mountainous regions of SA. Country scale AQ analysis was based on megacity and city scale data as well as selected areas of major industrial activity. The analysis period was 01st March–30th April 2020, which includes approximately 3 weeks of data prior to the implementation of COVID-19 restrictions and 5 weeks of continuous data under more complete national lockdowns. Exact dates for lockdown implementation varied from country to country (see Table 1) with most SA countries having implemented restrictions approximately from the third week of March.

To maintain consistency the period 1st–20th March was selected as the pre-lockdown period, with the 25th March to 30th April period was designated as the lockdown period. Selected satellite data for 2020 in general and the study period in particular were compared with available data from 2000–2019. To reduce the influence of missing values in daily satellite measurements (e.g., as a result of cloud cover, data quality thresholds and limitations in swath areas) available data

Table 1. List of lockdown implementation timeline in different countries.

Country	Lockdown Implementation Timelines (March)
Afghanistan	Gradual implementation of city based restrictions from the 22nd. Kabul fully locked down on the 28th.
Bangladesh	Complete lockdown started on 26th.
India	Curfew on 22nd followed by partial lockdown and complete lockdown on 25th.
Myanmar	Some restrictions and social distancing but no official national lockdown announced.
Nepal	Nepal implemented complete lockdown on 23rd.
Pakistan	Implemented lockdown in major cities between 22nd–24th.

was converted to a 5 days rolling mean for use in this study (e.g., Bechle *et al.*, 2013; Engel-Cox *et al.*, 2004).

2.1 Observation from Space

Most SA countries have limited ground-based observations of air pollutants (Martin *et al.*, 2019; Saikawa *et al.*, 2019) and any available in-situ observations are not representative for the entire region. To overcome this, multiple satellite based remote sensing products were used (Martin, 2008) along with available in-situ data.

2.1.1 Moderate Resolution Imaging Spectroradiometer (MODIS)

The Terra and Aqua Satellite platforms were launched in 1999 and 2002 respectively in solar-synchronous polar orbits. They are equipped with MODIS multispectral instruments providing continuous measurements of aerosols/clouds. In this study Level 2 (MOD04_L2) and Level 3 (MOD08D3), collection 6.1 aerosol products at 0.55 μm were used (1st March to 30th April for 2000 to 2020). The spatial resolution of L2 and L3 products is 10 km (at nadir) and 1° × 1°, respectively. The accuracy of MODIS AOD products over land is estimated to be within 0.05 ± 0.2 AOD (Kaufman *et al.*, 1997). Validation analysis of collection 6.1 products over the SA and Indian regions also showed a good agreement with AERONET observations (Bhattarai *et al.*, 2019; Mangla *et al.*, 2020; Wei *et al.*, 2019a, b). MODIS active fire products were also used to provide the timing and spatial distribution of large scale fires in the region (Giglio *et al.*, 2003; Justice *et al.*, 2002).

2.1.2 Ozone Monitoring Instrument (OMI)

The OMI system aboard NASA's Aura spacecraft was placed in a sun-synchronous polar orbit in 2004. It is a nadir-viewing instrument and measures backscattered solar radiation in the 0.27–0.5 μm wavelength range with a spectral resolution of 0.42–0.63 nm. This backscatter is used to derive column densities of different criteria pollutants including NO_2 and SO_2 at a resolution of 13 km × 24 km at nadir (Levelt *et al.*, 2006). The instrument has a 2600 km wide swath at the earth's surface and a local afternoon equator crossing time of 13:45. In this study Level-3 daily gridded NO_2 product (OMNO2d) binned and averaged into 0.25 × 0.25 degree global grids was used (see Haq *et al.*, 2015). Only total column NO_2 with a cloud fraction less than 30% was used (for a detailed analysis of the version-3 OMI NO_2 product see Krotkov *et al.*, 2017). For SO_2 the Level-3 daily global SO_2 data product (OMSO2e), based on the Band Residual Difference (BRD) algorithm was used (see Krotkov *et al.*, 2006). Each grid point contained one observation of SO_2 total column density for the Planetary Boundary Layer (PBL). This data point was selected from all good Level-2 pixels that overlap the study grid, excluding observations affected by row anomalies according to the method described in Jabeen *et al.* (2019) and Mallick *et al.* (2019).

2.1.3 TROPOspheric Monitoring Instrument (TROPOMI)

TROPOMI is a spectrometer launched on the Sentinel-5 Precursor (S-5 P) mission as a single-payload satellite in a sun-synchronous orbit by the European Space Agency. TROPOMI covers the ultraviolet (UV), visible (VIS), near-infrared (NIR) and shortwave infrared (SWIR) ranges (Veefkind *et al.*, 2012). with a daily global coverage at a spatial resolution of 7 × 7 km^2 with a swath of 2600 km. Total column density of CO is derived from the measurement of Earth's radiance spectra in the 2.3 μm spectral range of the shortwave infrared (SWIR) region (Fu *et al.*, 2016; Landgraf *et al.*, 2016). This study used the Level 3, Offline (OFFL) CO dataset for 2019 and 2020 (limited due

to age of satellite) from the Google Earth Engine platform data catalog (Gorelick *et al.*, 2017). Initial validation of TROPOMI CO data was shown to have a good agreement with the Copernicus Atmosphere Monitoring Service (CAMS) dataset over the Asian region (Borsdorff *et al.*, 2018).

2.2 Ground-Based Observations

2.2.1 US embassy surface air quality observations

The United State (US) Department of State (DOS) and the United State Environmental protection agency (U.S. EPA) collectively monitor AQ from U.S. embassies and consulates globally. Measurements follow federal reference or equivalent monitoring methods approved by the U.S. EPA. Data from these monitoring stations is made accessible via the DOS AirNow platform. Embassy hourly $PM_{2.5}$ data for 9 cities (Kabul, Islamabad, Lahore, New Delhi, Kathmandu, Kolkata, Dhaka, and Yangon) for the 1st March to 30th April period were used in this study (Fig. S1).

2.2.2 Nepal AQ data

Particulate matter (PM) measurements over Nepal (see 3.5) from an urban site in the Kathmandu city centre (Ratnapark established in 2016) and a semi-urban site in Kavre (Dhulikhel, established in 2017; also background site for Kathmandu) were used for this study. Both sites were established by the International Centre for Integrated Mountain Development (ICIMOD) in collaboration with the Government of Nepal's Department of Environment (DoEnv) (see Mahapatra *et al.*, 2018). Date used was real-time PM_{10}, $PM_{2.5}$, PM_1 at 60 Hz from a laser scattering instrument (Environmental Dust Monitor-180, Grimm Aerosol Technik GmbH, Germany) and meteorological parameters (WS700-UMB smart weather sensor, Lufft, Germany).

2.2.3 AErosol RObotic NETwork dataset (AERONET)

AERONET , Version 3 Level 1.5 AOD data at 500 nm was used from sites at Bidur, Pokhara, and Kyanging Gompa to understand the aerosol variation in high altitude regions of Nepal (Holben *et al.*, 1998). These sites were strategically chosen to study the transport of pollutants from low lying plains into high mountains areas through valleys. Here, Bidur and Pokhara represent two valley sites and Kyanging Gompa represents a high mountain site just below the Yala glacier in Nepal. Details of measurements carried out by the group at Yala glacier can be seen in Gul *et al.* (2021) and Rai *et al.* (2019).

3 RESULTS AND DISCUSSION

3.1 Sources of Pollution in South Asia

Air pollution across the SA region can be attributed to a wide range of natural and anthropogenic emission sources which show significant variations at a range of temporal scales. The impact of COVID-19 driven restrictions on AQ requires the understanding of existing emission scenarios over the study domain. For this, anthropogenic and open burning emission from the Regional Emission inventory in Asia (REAS3.1) and Global fire emission database (GFED) were analysed over the study domain to estimate the share of various emission sources typical for the months of March and April period (Kurokawa and Ohara, 2019; van der Werf *et al.*, 2017). National and regional scale emission inventories are limited for Asian countries as no country except Japan is legally required to submit annual national emission inventories under the UNFCCC or similar conventions (Janssens-Maenhout *et al.*, 2015; Kurokawa and Ohara, 2019). As a result of which emission estimates from SA are primarily based on individual project-based emission inventories. These individual project-based emission inventories are spatially and temporally discontinuous and as a result are a known source of uncertainty in regional emission inventories. Table 2 shows the relative share of major emission sectors for three major pollutants ($PM_{2.5}$, NO_x, and CO) over SA for March and April (emission data for year 2015 is used for this analysis). Open fires and the residential sector were major contributors to $PM_{2.5}$ and CO emissions for these months. The residential sector contributed 29% to $PM_{2.5}$ emission and 35% to CO emission. Over the domain 43% of $PM_{2.5}$ emissions and 32% of CO were attributed to open fire burning, the majority of which is forest fire though there is a significant contribution from agricultural waste burning. Studies

Table 2. Percentage contribution of major emission source sector over the south Asia domain during March and April months. It is estimated with REAS3.1 anthropogenic emission inventory and GFED fire database for the year 2015.

	Industrial	Transport	Energy	Residential	Open burning
$PM_{2.5}$	17	4	8	29	43
NO_x	15	37	31	6	11
CO	21	9	1	35	32

have identified the residential sector as the largest regional source of primary aerosol as an annual average (Lelieveld *et al.*, 2015) but for the pre-monsoon season, the relative share of emissions from forest fires and open biomass burning dominates other sources (Jena *et al.*, 2015). As Myanmar experiences widespread forest fires during the pre-monsoon season this is expected to play an important role in affecting the regional pollutant levels during the lockdown period. A study in the pre-monsoon season (undertaken between 18th March 2006 to 11th May 2006) reported that BC emission from biomass burning in SA were higher than those from anthropogenic sources (327 Gg and 203 Gg respectively). For this period Myanmar accounted for ~80% of all fire activity (Kumar *et al.*, 2015). For Nepal open burning is reported as the biggest source annually (> 50%) and the residential sector the second biggest source of $PM_{2.5}$ and CO (Shrestha, 2018). The transport and energy sectors are a small proportion of $PM_{2.5}$ and CO emissions (combined 12% and 10% respectively, Table 2). It is important to note here that residential emissions, a major source of $PM_{2.5}$ and CO, were not restricted through lockdown guidelines so is not expected to change significantly. The effects of pre lockdown migration or people movement associated with COVID-19 was not considered in detail in this study.

The transport sector, industrial emission, and the energy sector are major sources for NO_x emission over SA with 35%, 31%, and 15% share of total emissions respectively in March and April, compared with 44% and 52% for Europe and USA and 29% (Crippa *et al.*, 2018). Lockdown enforced restrictions included industrial and transport activities, however, relaxation of regulation was also provided for the supply and production of essential and emergency services, so emissions from this sector are also not expected to be zero. This large-scale decrease in economic activity also resulted in a reduction in power demand with approximately 12.0%, 28.6%, 18.3%, and 26.1% reduction (peak power demands) reported in Bangladesh, Bhutan, Nepal, and India, respectively (Agrawa *et al.*, 2020). In response to the reduction in power demand, renewable energy was given priority over coal-based power plants in part due to their marginal cost of production (statement by, Tim Buckley, IEEFA's Energy Finance studies) which is expected to reduce emissions from the energy sector during the lockdown. A significant reduction in re-suspended dust and construction dust was also expected due to restrictions on vehicular traffic and construction activities. However, on-road re-suspended dust, construction dust, and industrial dust are major contributors in cities and industrial zones and are not included in the emission inventories (Guttikunda *et al.*, 2019; Philip *et al.*, 2017). From the emission data it could be broadly expected that a strict lockdown would bring substantial reductions in NO_x levels whereas mitigation of the residential sector and control of forest fires would be required for a significant reduction in $PM_{2.5}$ and CO levels.

3.2 Impact of Lockdown on the Air Quality of South Asia

From the existing literature it can be seen that across SA, pollutant levels tend to be higher in April compared to March. Therefore, this study analyses the change in AQ due to lockdown in three ways (a) comparison of AQ during lockdown with long-term datasets, (b) comparison of AQ during lockdown with the AQ in the pre-lockdown period in 2020, (c) The impact of lockdown on annual intraseasonal trends in AQ for the entire study period. Long-term data sets used in the analysis includes the available data sets for the previous years for each pollutant.

3.2.1. Comparison of lockdown period (2020) mean with historical long-term mean

Fig. 1 (left panel) shows the long-term mean (years preceding 2019) satellite-derived columnar AOD, NO_2, SO_2, and CO over SA for the lockdown period (25 March–30 April). An understanding

ORIGINAL RESEARCH
https://doi.org/10.4209/aaqr.210376

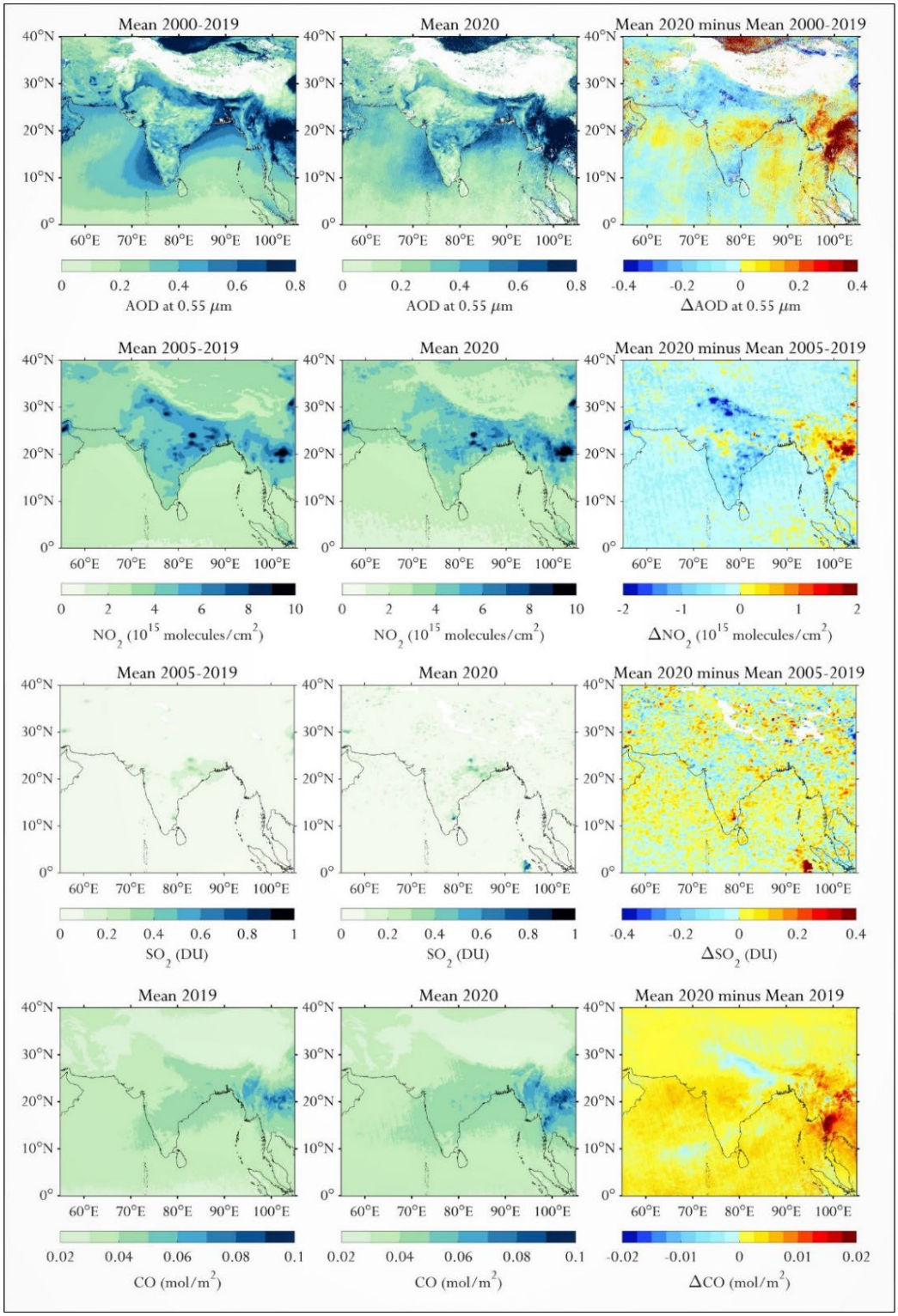


Fig. 1. (Left) Long-term mean of AOD (2000–2019), NO_2 (2005–2019), SO_2 (2005–2019) and CO (2019) during the 25th March–30th April lockdown period over south Asia. (Middle) AOD, NO_2, SO_2, and CO for 2020 over south Asia during the 25th March–30th April lockdown period. (Right) Difference between 2020 AOD, NO_2, SO_2 and CO compared to their long-term mean.

of the spatial distribution of the pollutants across SA during this period in previous years was deemed necessary to examine the impact of lockdown imposed in 2020. The mean for the year 2020 (Fig. 1, middle panel) represents the mean during the COVID-19 forced lockdown period, and

the difference between long-term mean and 2020 means displays the changes due to lockdown (Fig. 1, right panel).

Long-term data shows that AOD was usually high over the IGP and eastern part of the SA domain due to its high population density, residential and industrial emissions and forest fires (Fig. 1). In general, the AOD over IGP also remains high throughout the year and exhibits a west to east transition depending on the seasons (Dey and Di Girolamo, 2011). High aerosol loads often penetrate the surrounding Himalayan foothills and high mountain regions lying North of the IGP, which has also been observed in earlier studies (Rupakheti *et al.*, 2017). These mountainous regions in the North are also influenced by emissions of seasonal forest fires (Mehra *et al.*, 2019). AOD gradually decreases while moving towards the South of the IGP with few patches of high loading in the central and eastern regions of India. In contrast to widely distributed AOD over SA, NO_2 and SO_2 are localized to distinct hotspots. High NO_2 levels are found over cities primarily owing to vehicular emissions, whereas high SO_2 levels are observed over industrial zones and power plant locations. Open burning also contributes to 11% of total NO_2 emission over SA hence NO_2 hotspots are also observed in the forest fire dominated eastern part of the SA domain. High CO levels are seen in the eastern side of the SA domain including Myanmar, Bangladesh and the Eastern states of India (Fig. 1). Such high CO levels in these regions are attributed to the frequent forest fire activity during the pre-monsoon season (Girach and Nair, 2014). Over SA, the long-term mean of columnar AOD, NO_2, and CO during the lockdown period was 0.41 (0.40–0.42, 95% CI), 3.35×10^{15} (3.33×10^{15}–3.37×10^{15}, 95% CI) molecules cm^{-2}, and 0.033 (0.32–0.33, 95% CI) mole m^{-2} respectively. While that for the year 2020 was 0.42 (0.40–0.44, 95% CI), 3.77×10^{15} (3.69×10^{15}–3.84×10^{15}, 95% CI) molecules cm^{-2} and 0.0346 (0.343–0.349, 95% CI) mole m^{-2} respectively. However, SO_2 means for this large domain from OMI are near zero (Krotkov *et al.*, 2016).

The spatial mean of AOD, NO_2, and CO over SA during the lockdown period show an increase of 2.6%, 12.6%, and 5% respectively in 2020 compared to the long-term means. Fig. 1 shows marked heterogeneity (Table 3, Fig. 1). The decrease in AOD is higher over the IGP, ranging from approximately 0.1 to 0.4; this accounts for a 20 to 80% decrease in AOD. However, in the same period, an increase of AOD from 0.2 to 0.4 was observed in the eastern part of the domain; this is approximately a 20–60% increase over the long-term mean of this period. Similar to our findings, a decrease of 46% in AOD over North India and 42% in the Eastern IGP during the lockdown period compared to the 3 year mean using satellite data sets was reported by Kant *et al.* (2020). Reduction in anthropogenic emissions due to restricted activities is main reason for decrease in AOD over IGP, whereas forest fires is responsible for increase in AOD over eastern part of the domain. CO levels in the year 2020 indicate an increase in most of the region, whereas some decrease was observed over the IGP. NO_2 was shown to have decreased by ~20% over the majority of the region, while in the Eastern part an increase of ~20–40% was observed.

The spatial heterogeneity in patterns of decrease or increase of pollutants compared to their long-term mean over the region and at country-level were also studied. Changes in AOD, NO_x, and CO during the lockdown period compared to their long-term mean over individual SA countries was shown to have significant variation (Table 3) with 8%, 15%, and 24% decreases in AOD over India, Bangladesh, and Pakistan and an increase of 15% in Myanmar. An increase in mean AOD over India from 0.35 to 0.39 was reported for the year 2020 compared to the year 2019 (Pathakoti *et al.*, 2020). This can be attributed to interannual variability so a comparison with long-term mean is expected to provide a more robust tool in the analysis of effect of lockdown on AQ. A significant reduction in AOD with respect to its long-term mean was reported over India (Ranjan *et al.*, 2020)

Table 3. Percentage change in AOD, NO_2, and CO level over the south Asia domain and major countries during the 2020 lockdown period compared to their long-term means. The 95% confidence interval for the percentage change is given in parenthesis.

Sl. No.	Region	AOD	NO_2	CO
1.	South Asia domain	2.6 (–0.1–5.3)	12.6 (12.0–13.2)*	5.1 (4.5–5.6)*
2.	Pakistan	–24.3 (–26.7 to –22.0)*	–9.2 (–10.3 to –8.1)*	2.6 (2.0–3.1)*
3.	India	–8.6 (–10.4 to –7.0)*	–10.0 (–10.6 to –9.5)*	4.4 (3.8–4.9)*
4.	Bangladesh	–15.8 (–18.7 to –12.9)*	–4.1(–6.1 to –2.0)*	1.8 (0.9–2.7)*
5.	Myanmar	15.4 (10.6–20.2)*	1.8 (–4.1–7.9)	7.5 (5.1–9.8)*

* represents statistically significant change with p-value < 0.05.

ORIGINAL RESEARCH
https://doi.org/10.4209/aaqr.210376

which was similar to our finding for India. Similarly, a 4–10% decrease in NO_2 level was observed for India, Bangladesh, and Pakistan whereas a slight increase of 2% was observed over Myanmar. A 17% reduction in NO_2 over India for March 2020 compared to the 10-year mean was reported and attributed to COVID-19 driven lockdowns (Metya *et al.*, 2020).

3.2.2 Comparison of pre and during lockdown period in 2020

Satellite-derived data for AOD, NO_2, SO_2, and CO during lockdown was compared with that of the pre-lockdown period (Figs. 2 and 3). On the regional scale (over SA) AOD, NO_2, and CO

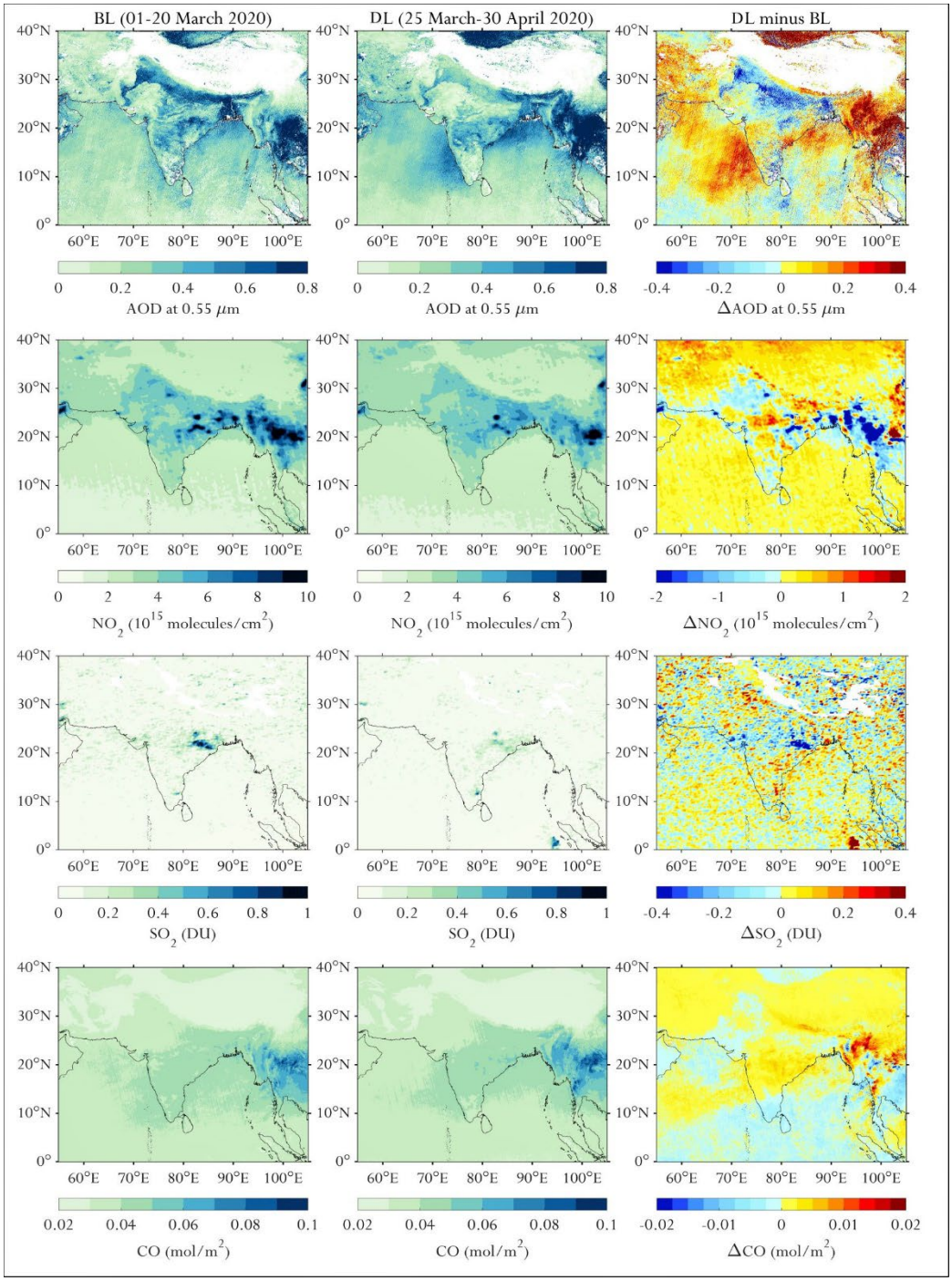


Fig. 2. AOD, NO_2, SO_2 and CO burden over south Asia during lockdown (Middle) and pre-lockdown periods (Left). The difference between AOD, NO_2, SO_2, and CO for pre-lockdown and during lockdown period (Right). Here, BL and DL represents before lockdown and during lockdown period.

ORIGINAL RESEARCH
https://doi.org/10.4209/aaqr.210376

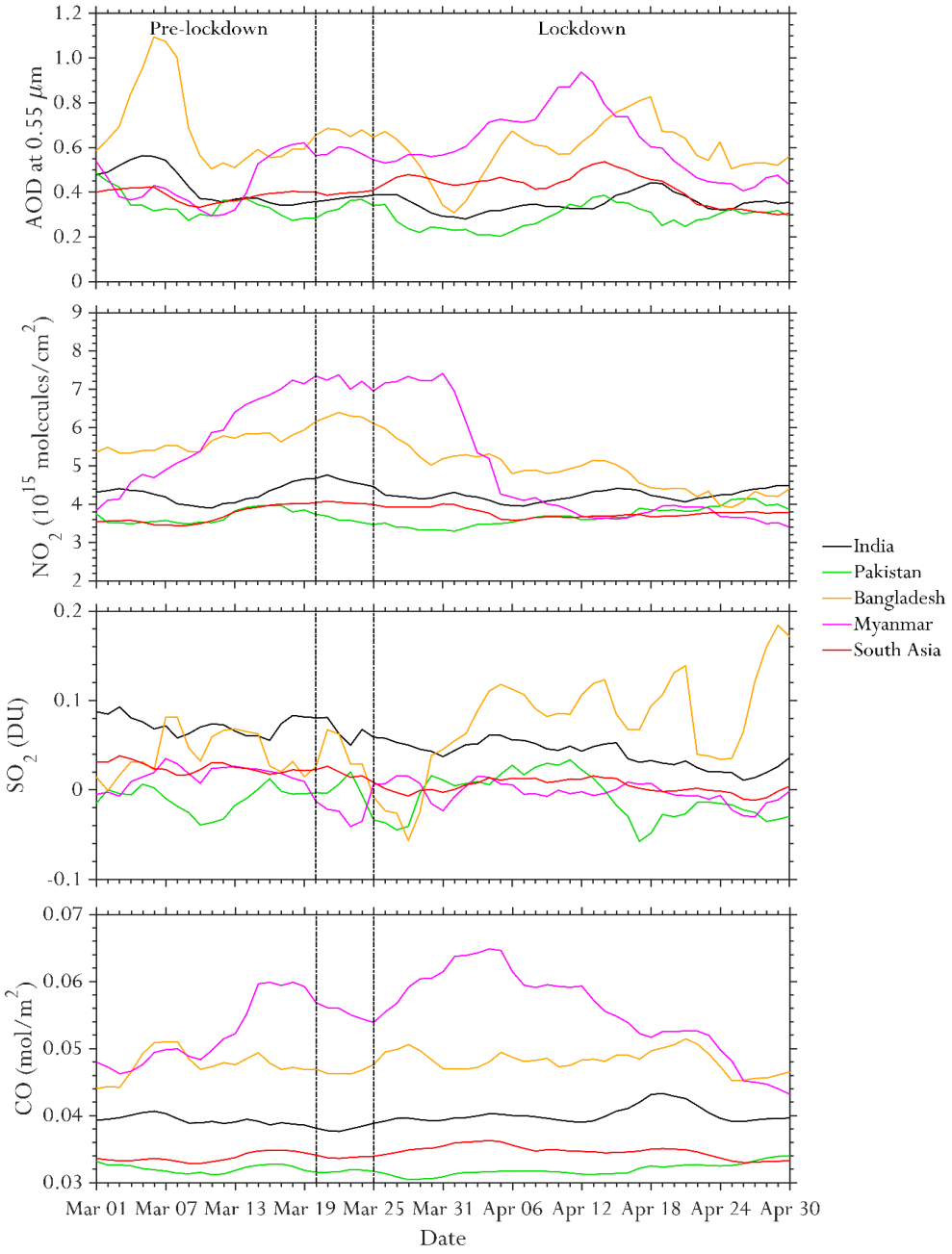


Fig. 3. Line plot for a daily mean of AOD, NO_2, SO_2, and CO over south Asia, India, Pakistan, Bangladesh, and Myanmar from 1 March 2020 to 20 April 2020. The vertical lines are representing the buffer zone between the pre-lockdown period (01 March–20 March) and lockdown period (25 March to 30 April) considered in this study.

indicate an increase of 9.5%, 2%, and 2.6%, respectively, during the lockdown period compared to the pre-lockdown in 2020 (Table 4). During the lockdown period, the AOD level over the IGP region decreased (relative to pre lockdown values) while an increase was observed in the Eastern part of the domain and Northern mountain regions. A decrease in AOD for IGP, north-west and east India, and increase over central India during the lockdown period was also observed in another study that used both MODIS terra and MODIS aqua data (Pandey and Vinoj, 2021). A reduction in NO_2 levels was observed over the majority of the SA region but a substantial increase was observed in the Eastern area. An increase in NO_2 was also observed in the mountainous region along the Northern side of the IGP, with patches of high NO_2 also observed in central India; an area of significant industrial activity, with a number of power generation plants, and significant

Table 4. Percentage change in AOD, NO_2, and CO level during lockdown period compared to the pre-lockdown period for the south Asia domain and countries (Pakistan, India, Bangladesh, and Myanmar) for year 2020. The 95% confidence interval is given in parenthesis.

Sl. No.	Region	AOD	NO_2	CO
1.	South Asia domain	9.5 (1.5–1.5)	2.0 (–0.4–4.3)	2.6 (1.3–3.9)
2.	Pakistan	–15.6 (–24.1 to –7.1)	0.0 (–3.3–3.3)	–0.5 (–1.8–0.8)
3.	India	–18.3 (–25.7 to –10.8)	–0.7 (–3.0–1.6)	2.1 (0.6–3.6)
4.	Bangladesh	–14.4 (–26.1 to –2.6)	–13.8 (–18.2 to –9.3)	1.2 (–0.8–3.2)
5.	Myanmar	39.8 (23.1–56.4)	–17.7 (–30.6 to –4.8)	6.2 (0.1–12.2)

mining activity. The CO spatial distribution shows an increase over the majority of the region with a higher increase in the eastern part. More CO was seen in the forest fire-dominated regions in the Eastern part of the domain which was seen to spread to the majority of the region due to the rapid mixing and transport of CO coupled with its atmospheric lifetime. For SO_2 a decrease was reported only over the industrial gridded areas, while other regions did not show any clear evidence of change.

Country-specific line plots from running averages of pollutants from satellite data are shown in Fig. 3. These clearly show the variation reported for the pre and post lockdown phase compared to SA. For Myanmar, the AOD and CO data showed sustained growth in levels during the lockdown phase that can be attributed to forest fires over this region (Fig. 4). A decline in NO_2 levels during lockdown was observed to be consistent in majority of the countries attributing to lower vehicular emissions. An increase in levels of CO was observed in all countries except Pakistan linked to increased forest fire and biomass burning activity. It indicates the possible influence of change in meteorological parameters (like relative humidity, temperature, and solar insolation) and variations in forest fire emission from March to April. These changes again indicated that with prohibitions on vehicular activity and industrial operations, the level of pollutant reduction at a regional scale is not even close to 50%, indicating the presence of other important emission sectors (e.g., residential or open burning sources). From this analysis it is clear that a focus on mitigation has to be concentrated on the dominant and cost-effective sectors, at least in this season.

3.2.3. Comparison of the pre and during lockdown trends for 2020 and selected long-term dataset

Daily mean of AOD, NO_2 and CO obtained with historical long-term datasets over SA shows an increasing trend during the study period (01st March–30th April); similarly, individual countries also indicate an increasing trend. Such a variation might be attributed to the increase in forest fire, agricultural waste burning of rabi crop, and frequent dust episodes prevalent during the dry season (Sadavarte *et al.*, 2016; Yadav *et al.*, 2017). The dry season (pre-monsoon) also experiences high winds that favors the transport of dust which contributes to the entire AOD column (Madineni *et al.*, 2021). The influence of relative humidity and favorable meteorological conditions might also be probable causes of AOD enhancement reported over central India (Pandey and Vinoj, 2021). The long-term data in this study suggests an increase of 12.5%, 4.9%, and 3.6% in AOD, NO_2, and CO, respectively during the lockdown time compared to the pre-lockdown time over SA (Table 5). However, in the year 2020, the percentage increase in AOD, NO_2, and CO over SA is restricted to 9.5%, 2.0%, and 2.6% respectively during the lockdown in comparison to the pre-lockdown period (Table 4). The lower percent increase of AOD, NO_2, and CO during 2020 compared with the long-term data could be attributed to the effect of lockdown implemented over the region. In a similar analysis for individual countries, Pakistan, India, and Bangladesh AOD values declined by 15.6%, 18.3%, and 14.4% respectively during the lockdown period in comparison to the pre-lockdown period (Table 4). But the same in long-term data increased by 13.6%, 8.2%, and 14.4% for Pakistan, India, and Bangladesh respectively (Table 5). On the contrary, AOD values for Myanmar indicated an increase of 39.8% during the lockdown period in comparison to the pre-lockdown phase, and a 24.3% increase was seen with long-term datasets. This can be interpreted as the net decrease of 26–30% over India, Pakistan, and Bangladesh, 15.4% increase over Myanmar, and the net decrease over SA domain by 3%. The decline in the NO_2 trend is also observed for SA as

Table 5. Percentage change in AOD, NO_2, and CO level during previous years lockdown period (25th March–30th April) compared to the previous years pre-lockdown period (1st March–20th March) with their long-term dataset (2000 to 2019 for AOD, 2005 to 2019 for NO_2 and 2019 for CO) for south Asia and major countries. The 95% confidence interval for the percentage change is given in parenthesis.

Sl. No.	Region	AOD	NO2	CO
1.	South Asia domain	12.5 (9.5–15.5)	4.9 (3.9–5.9)	3.6 (2.4–4.8)
2.	Pakistan	13.6 (10.7–16.6)	8.1 (6.9–9.4)	2.3 (1.3–3.3)
3.	India	8.2 (6.6–9.9)	4.2 (2.8–5.7)	3.3 (2.3–4.3)
4.	Bangladesh	15.4 (12.9–18.0)	–7.2 (–10.2 to –4.2)	6.2 (3.7–8.7)
5.	Myanmar	24.3 (16.1–32.5)	–10.6 (–2.1 to –19.1)	17.0 (11.9–22.1)

well as for Pakistan, India, Bangladesh, and Myanmar (Tables 4 and 5). Over SA, mean CO showed an increase of 2.5% while that for India and Bangladesh increased by 2% and 1% respectively. Whereas for Myanmar it increased by 5% and in Pakistan, it remained almost unchanged with a slight decrease of 0.5%.

The share of different emission sources varies among the individual countries, which is one of the major factors in determining the impact of lockdown on the AQ (Venter *et al.*, 2020). Cities of China and the USA have shown variations in the impact of lockdown and similarly, the variation is also reported in China and India (Metya *et al.*, 2020; Shakoor *et al.*, 2020). Such variability can be attributed to variation in emission share from different sectors of China and the USA and also the extent of lockdown. The share of residential emission is large, and it is widely distributed over the SA region. Hence, complete mitigation of the residential sector emission in South Asian countries can achieve considerable improvement in AQ regionally (Lelieveld *et al.*, 2019; Upadhyay *et al.*, 2018). Simulations with zero-out emission sectors for the globe predicted that removing transport sector emission will reduce $PM_{2.5}$ concentration by 6–7% in India, East Asia, and Southeast Asia whereas it reduces 27–28% $PM_{2.5}$ in North America and Europe (Silva *et al.*, 2016). Whereas phasing out residential and commercial sector emission will reduce 42% of $PM_{2.5}$ in India and 10% and 20% $PM_{2.5}$ reduction in North America and Europe (Silva *et al.*, 2016). However, we don't expect any considerable change in residential sector emission and hence significant reduction at the regional scale is not observed in the SA region. In general, India has spent approximately $ 13.7 billion $year^{-1}$ on emission control of which 80% was spent on the transportation sector whereas the cost of LPG and similar subsidy activities is $ 6 billion per year (Cameron *et al.*, 2016; Purohit *et al.*, 2019). A recent study estimated that the reductions in household emission would allow the achievement of national ambient AQ standards for $PM_{2.5}$ (Chowdhury *et al.*, 2019). These studies performed over India indicate that the expenses for mitigation measures in transport, industrial sectors are higher than the residential sector, but the potential of air pollution reduction is higher in residential sector than the others. Hence, mitigation in residential sector emission is comparatively cost effective as well as efficient than mitigation measures for transport and industrial sector. It indicates that prioritizing emission control for particular sources can expedite the air pollution mitigation process.

A decline in pollutants level for Pakistan, India, and Bangladesh depicts the influence of lockdown-driven reduction in anthropogenic emission whereas the rise in Myanmar is reflecting the increase in forest fire emission during this period. Total fire count over South Asia increased from 2150 counts day^{-1} in the pre-lockdown period to 2359 counts day^{-1} during lockdown with a large-scale forest fire event were observed during 25th March to 06th April (Fig. 4). Residential sector emissions as a major contributor to CO remains almost unchanged during this period. So, forest fires as the other biggest contributor to CO levels was the most probable reason for such an increase.

3.4 Local-Scale Air Quality Analysis

From the above analysis, it was concluded that on a regional basis lockdown measures did not bring in a significant improvement in AQ. An analysis of various satellite and in-situ $PM_{2.5}$ data obtained from the US embassy at a city-scale over individual country capitals (Kabul, Islamabad, Delhi, Yangon, Thimphu, Kathmandu, and Dhaka) and major industrial grid in the SA region was

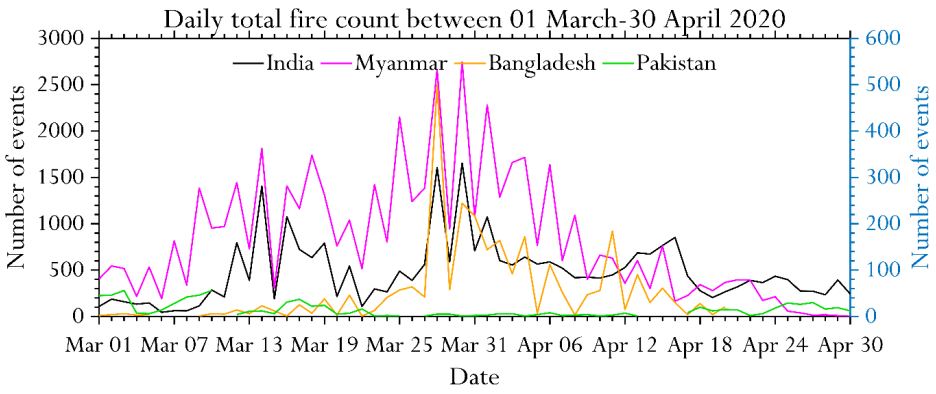


Fig. 4. Line plot of daily total MODIS fire counts over India, Pakistan, Bangladesh, and Myanmar with India and Myanmar on the right Y-axis, and Bangladesh and Pakistan on the left Y-axis.

undertaken. The industrial grid was chosen within India between 20.5–22.5 N and 81.5–85.5 E. This grid includes a number of coal (e.g., southeastern coal field limited, HIL coal mines, Hindalco coal mines), and other mines (like zink mines, stone mine, cement mines, metal mines), along with thermal power stations (Dr. Shyama Prasad Mukherjee thermal power station, Atal Bihari Vajpayee thermal power station, Jindal thermal power limited, Hasdeo thermal power station, Acbil thermal power plant, Hydel power plant). AQ for other industrial cities like Karachi in Pakistan, Singrauli and Jamshedpur in India, Hetauda in Nepal, and Chattogram in Bangladesh were also analyzed (Table 6). Mean AOD for the lockdown period was reduced by approximately 20% over Islamabad and New Delhi whereas a 15–20% reduction was seen in the selected industrial grid and Yangon. An approximate 10% decrease was observed over Dhaka. Cities with heavy vehicular loads like Dhaka and New Delhi showed substantial percentage reductions of approximately 39% and 21% in NO_2 burden. Compared to the 5-year mean of NO_2 over New Delhi a 54% reduction was observed in OMI NO_2 data (Pathakoti *et al.*, 2020) which were similar to those observed in the present study. Similar decline in NO_2 concentration during the lockdown period was shown for many cities across the world through satellite and ground-based observation (Sharma *et al.*, 2020b; Venter *et al.*, 2020; Wang *et al.*, 2020). A small percentage decrease (ranging between 0.5 to 3%) in CO levels was observed over Lahore, Islamabad, New Delhi, and Dhaka during the lockdown period compared to the pre-lockdown period. Kathmandu and Thimphu showed an increase in mean AOD, NO_2, and CO levels during the lockdown period compared to pre-lockdown. An increase in forest fire emissions during this period is considered to be the most

Table 6. Percentage change in mean AOD, NO_2, and CO during the lockdown period compared to their respective pre-lockdown period over select cities and the industrial grid based on satellite data. The final column shows the percentage change in $PM_{2.5}$ during the lockdown period compared to pre-lockdown at the US embassy monitoring stations. The 95% confidence interval is given in parenthesis.

City	AOD	NO_2	CO	$PM_{2.5}$
Kabul	28.6 (10.7–46.3)	2.9 (–2.3–8.0)	2.6 (1.1–4.1)	–50.3
Islamabad	–29.3 (–45.0 to –13.5)	–3.8 (–12.0–4.4)	–1.8 (–4.2–0.6)	–23.4
New Delhi	–38.5 (–50.4 to –26.5)	–21.2 (–28.3 to –14.1)	–2.4 (–5.3–0.6)	–35.4
Dhaka	–7.9 (–19.8–4.1)	–39.0 (–47.8 to –30.2)	–0.5 (–2.8–1.8)	–39.2
Kathmandu	45.0 (19.5–70.3)	10.3 (3.0–1.76)	18.3 (13.2–24.5)	–0.7
Thimphu	18.0 (3.1–32.9)	3.7 (–1.8–9.2)	5.4 (2.1–8.7)	
Yangon	–17.8 (–34.3 to –1.2)	–1.2 (–7.5–5.1)	–11.8 (–16.2 to –7.3)	–26.1
Industrial grid	–14.6 (–21.7 to –7.5)	–11.7 (–17.8 to –5.6)	6.4 (3.3–9.6)	
Karachi	–8.5 (–21.5–4.3)	–36.1 (–42.9 to –29.2)	–7.1 (–14.1–0)	
Jamshedpur	–25.3 (–37.9 to –12.7)	–3.7 (–13.5–6.1)	–12.1 (–16.1 to –8.1)	
Singrauli	–41.9 (–56.5 to –27.2)	8.7 (–12.7–30.2)	0.8 (–2.2–3.8)	
Hetauda	3.3 (–15.6–22.3)	16.9 (–0.4–34.3)	21.8 (16.1–27.4)	
Chattogram	40.6 (22.3–58.8)	–16.7 (–29.5 to –4.0)	–2.4 (–12.6–7.8)	

likely reason for this increase. Yangon and Mandalay showed contrasting trends for pollutants during the lockdown period. AOD and CO are decreased by 18% and 12% in Yangon. A small change (–1.2%) was observed for NO_2 over Yangon during the lockdown period compared to the pre-lockdown period. In contrast to other SA cities, only a small change in NO_2 level (–4 to 3% in comparison with 5-year mean) was observed for Yangon (Kanniah *et al.*, 2020). A 22% increase in AOD was observed over Kabul, which might have been due to increased particulate re suspension associated with dust transport in the pre-monsoon season. The selected industrial grid shows a decrease in levels of aerosol and gaseous pollutants as would be expected with reductions in industrial activity, combustion, heavy vehicle movement and lowering of coal-based power generation. This slowdown in industrial activity, limited vehicular movement and decreased power needs may have led to the 15% reduction in aerosol load and 12% reduction is NO_2 as observed during lockdown. An increase of 6% in CO levels over the same period could be the result of anecdotal reports of increased open burning. All the study cities except Dhaka and the industrial grid showed very low levels of SO_2. A 44% reduction in SO_2 was observed over Dhaka. SO_2 levels over the industrial grid were approximately 3–4 times greater than Dhaka and decreased by more than 50% during the lockdown period. A similar reduction of 17% for SO_2 was also reported over the identified power plant hot spot domain in east India during March compared to the 5 year mean SO_2 (Metya *et al.*, 2020). The industrial cities of Karachi, Jamshedpur and Singrauli experienced 8.5%, 25.2% and 41.9% reductions in AOD (respectively) whereas Chattogram and Hetauda exhibited 40.5% and 3.3% increases in AOD (Table 6). Karachi and Jamshedpur experienced reductions in SO_2, NO_2 and CO, however Hetauda experienced increases in all the selected AQ parameters, which could be associated with increased forest fire activity in the region.

In-situ observations of $PM_{2.5}$ from the US embassy monitoring stations suggest a substantial decrease at most of the sites except Kathmandu (Table 6 and S1). These stations are situated in big cities where the transport sector is a major source of air pollution. Comparison of mean $PM_{2.5}$ pre and during lockdown decreased by more than 50% over Kabul, Lahore, and Kolkata whereas over New Delhi and Dhaka a decrease of 35% and 39% respectively was observed. A reduction of over 50% in levels of particulate matter and considerable reduction in other pollutants were also reported from the CPCB, DPCC, and IITM observatories in New Delhi (CPCB, 2020; Mahato *et al.*, 2020). The increase in PBL height over majority of the study domain during lockdown period compared to pre-lockdown might also be one of the reasons for decrease in surface $PM_{2.5}$ along with decrease in anthropogenic emission (Madineni *et al.*, 2021; Zhang *et al.*, 2021). A substantial decrease of 23% and 26% was observed in Islamabad and Yangon for $PM_{2.5}$. At one of the two stations of Kathmandu almost no change was seen and at the other (Phora Durbar) a 25% increase in $PM_{2.5}$ was observed. The decrease in $PM_{2.5}$ observed at the Kabul monitoring station did not agree with the trend observed in MODIS columnar AOD but is consistent with the decline in anthropogenic activities. High dust emission in the pre-monsoon season might be the reason for increased columnar AOD over Kabul. While the rise in $PM_{2.5}$ at the US Embassy site in Kathmandu is consistent with forest fire activity (see Section 3.5). Similar results were also observed in studies performed over India and other major cities across SA (e.g., Kumar *et al.*, 2020; Sharma *et al.*, 2020a).

3.5 Mountain Region Analysis

Over the northern mountainous regions of SA, there was an increase in reported AOD during the lockdown period when compared to pre-lockdown. In this section, in-situ PM_{10} and $PM_{2.5}$ data from the Kathmandu and Kavre sites were used to further investigate this finding. Comparison of PM_{10} data for both the sites (Fig. 5) showed much higher values (close to three times) at the Kathmandu site (69.7 ± 41.1 μg m^{-3}) compared to the Kavre site (24.8 ± 10.2 μg m^{-3}) in the pre-lockdown period. While during lockdown, the PM_{10} concentration observed at Kathmandu site (37.3 ± 21.3 μg m^{-3}) was only 15% higher than that of Kavre site (32.3 ± 37.3 μg m^{-3}). This indicates that within the valley, a high concentration of PM_{10} generally exists (attributed to sources like re-suspended dust and construction activities) that reduced by ~46% during lockdown versus pre-lockdown. Comparison of pre-monsoon PM_{10} data from earlier study indicates an average of 241 ± 134 μg m^{-3} over Kathmandu (Putero *et al.*, 2015). These differences might exist due to the different pre-monsoon period definitions considered by Putero *et al.* (2015) that ranged from February to May and the location of the station. There are limited studies of PM_{10} variation from

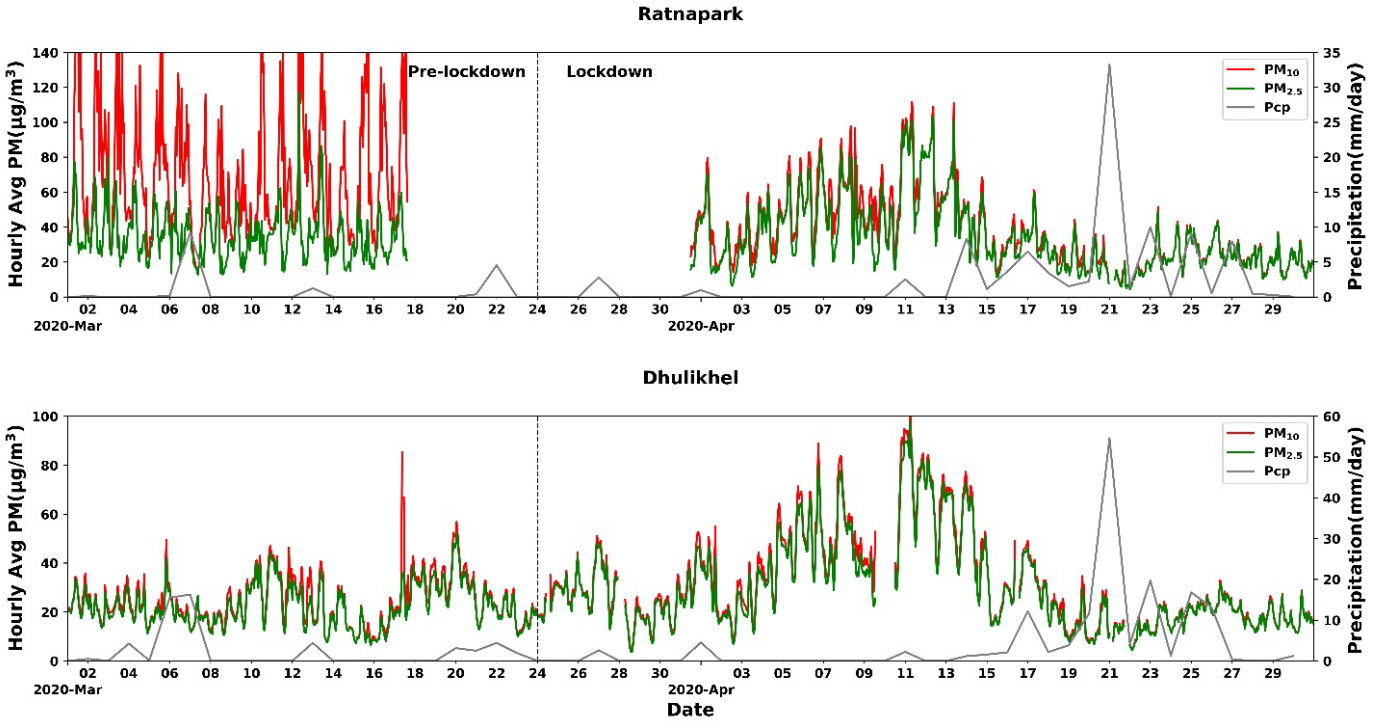


Fig. 5. Hourly variation in PM_{10} and $PM_{2.5}$ during the pre-lockdown and lockdown periods at the Kathmandu (Ratnapark) and Kavre (Dhulikhel) sites. Daily variation in precipitation rate (Pcp) is shown by the grey line and the right hand Y-axis.

within the valley with the notable exception of a study in 2008 (Aryal *et al.*, 2008) which is not directly comparable due to the expansion of Kathmandu between 2008 and 2021.

Comparison of $PM_{2.5}$ at both stations indicates that levels of $PM_{2.5}$ were ~55% higher at the Kathmandu site (35 ± 14 µg m^{-3}) compared to the Kavre site (22.5 ± 8.7 µg m^{-3}) during pre-lockdown. Similar values were also observed during studies from 2006–2007 but these comparisons are limited due to the age of these measurements (Aryal *et al.*, 2009; Stone *et al.*, 2010). Whereas the values at both the stations (33.2 ± 19.8 and 30.5 ± 18.6 µg m^{-3} for Kathmandu and Kavre sites respectively) were almost similar during the lockdown period. This indicates a stronger influence of sources such as transport, small scale industries and combustion within the valley region which then decreased during the lockdown period. However, a comparison of pre-lockdown and lockdown period $PM_{2.5}$ concentrations at both the stations indicate a gradual increase in $PM_{2.5}$ concentrations during the lockdown period reaching a maximum between the 5th–15th April 2020 followed by a rapid decline. This is contrary to findings from other studies on the impacts of lockdown on AQ (Collivignarelli *et al.*, 2020; Mahato *et al.*, 2020; Nakada and Urban, 2020; Sharma *et al.*, 2020b). The gradual increase in $PM_{2.5}$ could be strongly attributed to the simultaneous increase in forest fires in the nearby regions. This was supported by the time series plot of fire spots acquired from MODIS (25–35°E Latitude and 75–90°N longitude, i.e., encompassing the Kathmandu Valley, Fig. 6, bottom panel). During these events mean $PM_{2.5}$ concentrations were 51.2 ± 18.8 µg m^{-3} and 49.5 ± 22.2 µg m^{-3} (reaching 80–100 µg m^{-3} for few days) respectively at Kavre and Kathmandu. Similar impacts of forest fires on the ambient AQ in the region (during different years) have been reported at other sites in Nepal (Mehra *et al.*, 2019). Immediately after the forest fire events, increased rainfall events occurred over the study area which resulted in a rapid decline in PM levels associated with wet deposition. To study the effect of forest fires and rainfall on columnar aerosol loading over other locations in Nepal, AOD data from AERONET sites in Bidur, Pokhara, and Kyanging Gompa (Fig 6. Middle Panel) were also studied. Although these sites are geographically located in different ecosystems within Nepal, all indicated an increase in AOD values during forest fire events (along with increased $PM_{2.5}$ concentrations at the Ratnapark and Dhulikhel sites). There is evidence supporting the transport of emissions from forest fires up to the glaciers as high as 4000 masl in Nepal (Dhungel *et al.*, 2018; Gul *et al.*, 2021).

ORIGINAL RESEARCH
https://doi.org/10.4209/aaqr.210376

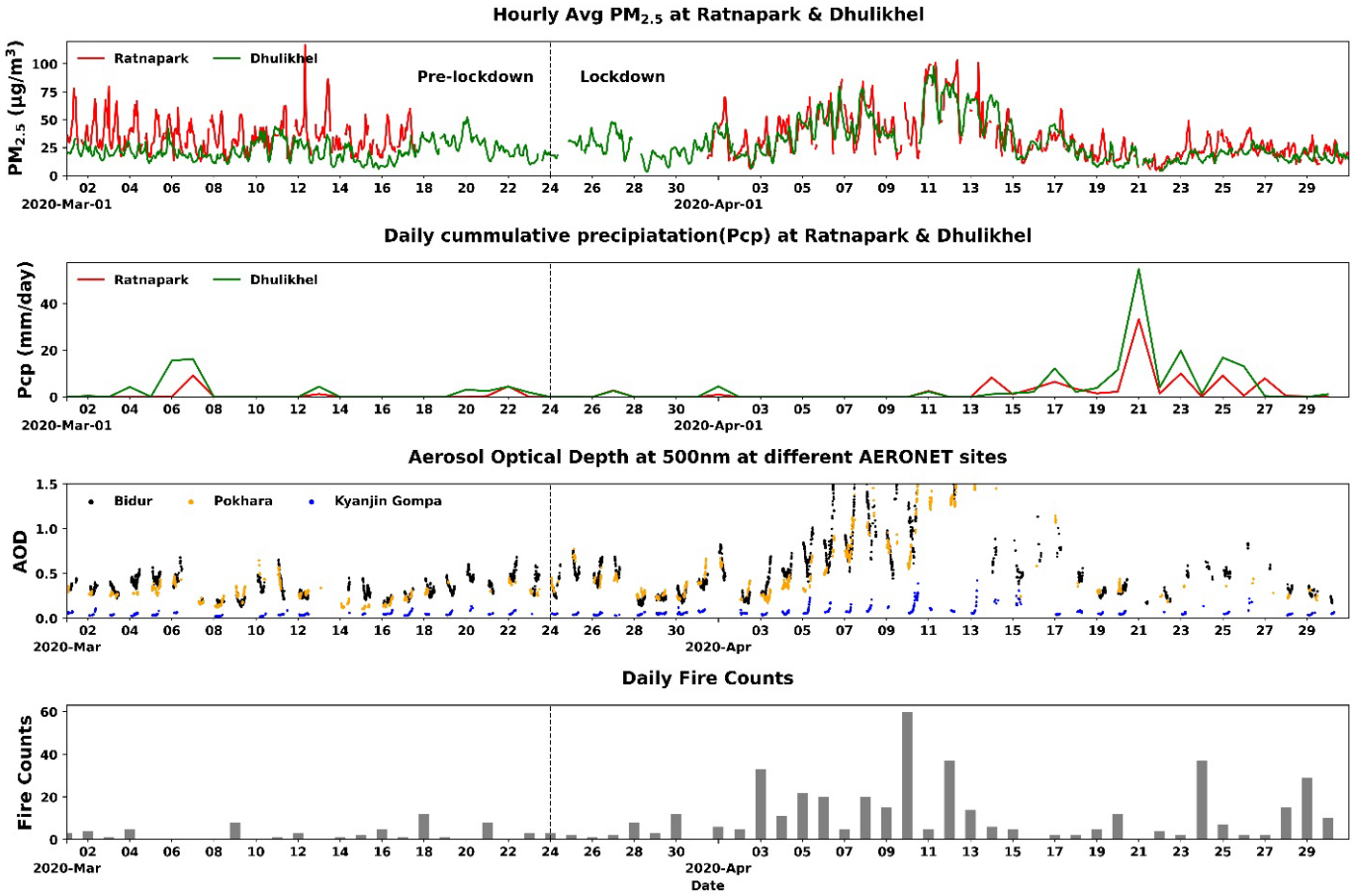


Fig. 6. (Top Panel) Hourly variation in $PM_{2.5}$ during the pre-lockdown and lockdown period at Kathmandu (Ratnapark) and Kavre (Dhulikhel), (Second from top) Daily precipitation at Kathmandu (Ratnapark) and Kavre (Dhulikhel), (Third from top) AOD from AERONET at three sites in Nepal with altitudinal variation, and (Bottom Panel) Daily fire counts.

Therefore, indicating that forest fire related emissions during this season plays an important role for high mountain regions in SA (which might have masked the effects of lockdown prompted emission reduction).

4 CONCLUSIONS

This study indicates that spatial means of AOD, columnar NO_2, and CO over SA during the defined lockdown period (25 March–30 April 2020) were 9.5%, 2.0%, and 2.6% higher than the pre-lockdown period (01 March–20 March 2020) and with the exception of CO. This change observed for the year 2020 is slightly lower than the change observed in the previous years pre lockdown and lockdown period, that can be attributed to the overall reduction due to lockdown. Country-level analysis indicates that during the lockdown a decline in AOD was observed for India, Pakistan, Bangladesh (~14–18%) while an increase was observed over Myanmar (~40%) and other mountainous regions in the North (i.e., Nepal). While for CO an increase in India, Bangladesh could be attributed to the effect of forest fires which dominated over the eastern region. NO_2 generally declined except for Pakistan where no change was observed. Satellite-based observations over country capitals indicate a mixed pattern of change but surface-based in-situ observation indicates an improvement in AQ (~20–60% $PM_{2.5}$ reduction) during the lockdown compared to the pre-lockdown phase. Overall, this study indicates that a reduction of vehicular and industrial emissions of the level seen during lockdown could lead to a reduction of fine particulate levels of approximately ~20–50% at the city level while on a regional scale that level of reduction might not be visible due to other strong contributing factors. Clearly reflecting the importance of other sources of emissions that are not directly linked to the large scale economic activity. This highlights

the need for a more detailed understanding of the spatiotemporal distribution of sources in different seasons for the effective design and implementation of air quality mitigation strategies. This also emphasize for a renewed focus on mitigation activities at the household level that is potentially cost effective, efficient and long term in nature. This study demonstrates the need for evidence-based action as opposed to anecdotal evidence or assumptions regarding solutions being the same across the region (e.g., targeting transport only). Such actions need to be based on in-depth cost-benefit analysis considering the sectoral contribution of commercial and domestic activity regionally. This will help to quantify benefits and define efficient and cost-effective actions to improve the quality of the air that we breathe.

ACKNOWLEDGMENTS

This study was partially supported by core funds of ICIMOD contributed by the governments of Afghanistan, Australia, Austria, Bangladesh, Bhutan, China, India, Myanmar, Nepal, Norway, Pakistan, Sweden, and Switzerland. The views and interpretations in this publication are those of the authors and are not necessarily attributable to ICIMOD. We would like to acknowledge Dr. Iqbal Mead, ICIMOD for his contributions in language editing and reviewing this manuscript. We are thankful to editor and two anonymous reviewers for their comments and suggestions to enhance the quality of this manuscript.

SUPPLEMENTARY MATERIAL

Supplementary material for this article can be found in the online version at https://doi.org/10.4209/aaqr.210376

REFERENCES

Agrawal, V.K., Panda, R.R., Parikh, J., Makwana, M. (2020). Impact of COVID-19 pandemic on South Asian Power Sector. May 2020. Integrated Research and Action for Development, India.

Aryal, R.K., Lee, B.K., Karki, R., Gurung, A., Baral, B., Byeon, S.H. (2009). Dynamics of $PM_{2.5}$ concentrations in Kathmandu Valley, Nepal. J. Hazard. Mater. 168, 732–738. https://doi.org/10.1016/j.jhazmat.2009.02.086

Aryal, R.K., Lee, B.K., Karki, R., Gurung, A., Kandasamy, J., Pathak, B.K., Sharma, S., Giri, N. (2008). Seasonal PM_{10} dynamics in Kathmandu Valley. Atmos. Environ. 42, 8623–8633. https://doi.org/10.1016/j.atmosenv.2008.08.016

Bechle, M.J., Millet, D.B., Marshall, J.D. (2013). Remote sensing of exposure to NO_2: Satellite versus ground-based measurement in a large urban area. Atmos. Environ. 69, 345–353. https://doi.org/10.1016/j.atmosenv.2012.11.046

Bhattarai, B.C., Burkhart, J.F., Stordal, F., Xu, C. (2019). Aerosol optical depth over the nepalese cryosphere derived from an empirical model. Front. Earth Sci. 7, 1–17. https://doi.org/10.3389/feart.2019.00178

Borsdorff, T., Aan de Brugh, J., Hu, H., Aben, I., Hasekamp, O., Landgraf, J. (2018). Measuring carbon monoxide with TROPOMI: First results and a comparison with ECMWF-IFS analysis data. Geophys. Res. Lett. 45, 2826–2832. https://doi.org/10.1002/2018GL077045

Cameron, C., Pachauri, S., Rao, N.D., McCollum, D., Rogelj, J., Riahi, K. (2016). Policy trade-offs between climate mitigation and clean cook-stove access in South Asia. Nat. Energy 1, 1–5. https://doi.org/10.1038/nenergy.2015.10

Chowdhury, S., Dey, S., Guttikunda, S., Pillarisetti, A., Smith, K.R., Di Girolamo, L. (2019). Indian annual ambient air quality standard is achievable by completely mitigating emissions from household sources. Proc. Natl. Acad. Sci. 116, 10711–10716. https://doi.org/10.1073/pnas.1900888116

Collivignarelli, M.C., Abbà, A., Bertanza, G., Pedrazzani, R., Ricciardi, P., Carnevale Miino, M. (2020). Lockdown for CoViD-2019 in Milan: What are the effects on air quality? Sci. Total Environ. 732, 139280. https://doi.org/10.1016/j.scitotenv.2020.139280

Central Pollution Control Board (CPCB) (2020). Impact of Lockdown (25th March to 15th April) on Air Quality, "Impact of Janta Curfew & Lockdown. Central Pollution Control Board, Ministry of Environment, Forest and Climate Change, Government of India, Delhi. https://cpcb.nic.in/openpdffile.php?id=TGF0ZXN0RmlsZS9fMTU4ODE1NjM0OF9tZWRpYXBob3RvMjEyNDEucGRm

Crippa, M., Guizzardi, D., Muntean, M., Schaaf, E., Dentener, F., van Aardenne, J.A., Monni, S., Doering, U., Olivier, J.G.J., Pagliari, V., Janssens-Maenhout, G. (2018). Gridded emissions of air pollutants for the period 1970--2012 within EDGAR v4.3.2. Earth Syst. Sci. Data 10, 1987–2013. https://doi.org/10.5194/essd-10-1987-2018

Dey, S., Di Girolamo, L. (2011). A decade of change in aerosol properties over the Indian subcontinent. Geophys. Res. Lett. 38, L14811. https://doi.org/10.1029/2011GL048153

Dhungel, S., Kathayat, B., Mahata, K., Panday, A. (2018). Transport of regional pollutants through a remote trans-Himalayan valley in Nepal. Atmos. Chem. Phys. 18, 1203–1216. https://doi.org/10.5194/acp-18-1203-2018

Engel-Cox, J.A., Holloman, C.H., Coutant, B.W., Hoff, R.M. (2004). Qualitative and quantitative evaluation of MODIS satellite sensor data for regional and urban scale air quality. Atmos. Environ. 38, 2495–2509. https://doi.org/10.1016/j.atmosenv.2004.01.039

Fattorini, D., Regoli, F. (2020). Role of the chronic air pollution levels in the Covid-19 outbreak risk in Italy. Environ. Pollut. 264, 114732. https://doi.org/10.1016/j.envpol.2020.114732

Fu, D., Bowman, K.W., Worden, H.M., Natraj, V., Worden, J.R., Yu, S., Veefkind, P., Aben, I., Landgraf, J., Strow, L., Han, Y. (2016). High-resolution tropospheric carbon monoxide profiles retrieved from CrIS and TROPOMI. Atmos. Meas. Tech. 9, 2567–2579. https://doi.org/10.5194/amt-9-2567-2016

Giglio, L., Descloitres, J., Justice, C.O., Kaufman, Y.J. (2003). An enhanced contextual fire detection algorithm for MODIS. Remote Sens. Environ. 87, 273–282. https://doi.org/10.1016/S0034-4257(03)00184-6

Girach, I.A., Nair, P.R. (2014). Carbon monoxide over Indian region as observed by MOPITT. Atmos. Environ. 99, 599–609. https://doi.org/10.1016/j.atmosenv.2014.10.019

Gorelick, N., Hancher, M., Dixon, M., Ilyushchenko, S., Thau, D., Moore, R. (2017). Google Earth Engine: Planetary-scale geospatial analysis for everyone. Remote Sens. Environ. 202, 18–27. https://doi.org/10.1016/j.rse.2017.06.031

Gul, C., Mahapatra, P.S., Kang, S., Singh, P.K., Wu, X., He, C., Kumar, R., Rai, M., Xu, Y., Puppala, S.P. (2021). Black carbon concentration in the central Himalayas: Impact on glacier melt and potential source contribution. Environ. Pollut. 275, 116544. https://doi.org/10.1016/j.envpol.2021.116544

Guttikunda, S.K., Nishadh, K.A., Jawahar, P. (2019). Air pollution knowledge assessments (APnA) for 20 Indian cities. Urban Clim. 27, 124–141. https://doi.org/10.1016/j.uclim.2018.11.005

Holben, B.N., Eck, T.F., Slutsker, I., Tanré, D., Buis, J.P., Setzer, A., Vermote, E., Reagan, J.A., Kaufman, Y.J., Nakajima, T., Lavenu, F., Jankowiak, I., Smirnov, A. (1998). AERONET - A federated instrument network and data archive for aerosol characterization. Remote Sens. Environ. 66, 1–16. https://doi.org/10.1016/S0034-4257(98)00031-5

International Centre for Integrated Mountain Development (ICIMOD) (2020). COVID-19 impact and policy responses in the Hindu Kush Himalaya. International Centre for Integrated Mountain Development, Kathmandu, Nepal. https://doi.org/10.53055/ICIMOD.2

Janssens-Maenhout, G., Crippa, M., Guizzardi, D., Dentener, F., Muntean, M., Pouliot, G., Keating, T., Zhang, Q., Kurokawa, J., Wankmüller, R., Denier Van Der Gon, H., Kuenen, J.J.P., Klimont, Z., Frost, G., Darras, S., Koffi, B., Li, M. (2015). HTAP-v2.2: A mosaic of regional and global emission grid maps for 2008 and 2010 to study hemispheric transport of air pollution. Atmos. Chem. Phys. 15, 11411–11432. https://doi.org/10.5194/acp-15-11411-2015

Jayarathne, T., Stockwell, C.E., Bhave, P.V., Praveen, P.S., Rathnayake, C.M., Islam, M.R., Panday, A.K., Adhikari, S., Maharjan, R., Goetz, J.D., DeCarlo, P.F., Saikawa, E., Yokelson, R.J., Stone, E.A. (2018). Nepal Ambient Monitoring and Source Testing Experiment (NAMaSTE): Emissions of particulate matter from wood- and dung-fueled cooking fires, garbage and crop residue burning, brick kilns, and other sources. Atmos. Chem. Phys. 18, 2259–2286. https://doi.org/10.5194/acp-18-2259-2018

Jena, C., Ghude, S.D., Pfister, G.G., Chate, D.M., Kumar, R., Beig, G., Surendran, D.E., Fadnavis, S., Lal, D.M. (2015). Influence of springtime biomass burning in South Asia on regional ozone (O_3):

A model based case study. Atmos. Environ. 100, 37–47. https://doi.org/10.1016/j.atmosenv.2014.10.027

Justice, C.O., Giglio, L., Korontzi, S., Owens, J., Morisette, J.T., Roy, D., Descloitres, J., Alleaume, S., Petitcolin, F., Kaufman, Y. (2002). The MODIS fire products. Remote Sens. Environ. 83, 244–262. https://doi.org/10.1016/S0034-4257(02)00076-7

Kanitkar, T. (2020). The COVID-19 lockdown in India: Impacts on the economy and the power sector. Glob. Transitions 2, 150–156. https://doi.org/10.1016/j.glt.2020.07.005

Kanniah, K.D., Kamarul Zaman, N.A.F., Kaskaoutis, D.G., Latif, M.T. (2020). COVID-19's impact on the atmospheric environment in the Southeast Asia region. Sci. Total Environ. 736, 139658. https://doi.org/10.1016/j.scitotenv.2020.139658

Kant, Y., Mitra, D., Chauhan, P. (2020). Space-based observations on the impact of COVID-19-induced lockdown on aerosols over India. Curr. Sci. 119, 539–544. https://doi.org/10.18520/cs/v119/i3/539-544

Kaufman, Y.J., Tanré, D., Remer, L.A., Vermote, E.F., Chu, A., Holben, B.N. (1997). Operational remote sensing of tropospheric aerosol over land from EOS moderate resolution imaging spectroradiometer. J. Geophys. Res. 102, 17051–17067. https://doi.org/10.1029/96jd03988

Krotkov, N.A., McLinden, C.A., Li, C., Lamsal, L.N., Celarier, E.A., Marchenko, S.V., Swartz, W.H., Bucsela, E.J., Joiner, J., Duncan, B.N., Boersma, K.F., Veefkind, J.P., Levelt, P.F., Fioletov, V.E., Dickerson, R.R., He, H., Lu, Z., Streets, D.G. (2016). Aura OMI observations of regional SO_2 and NO_2 pollution changes from 2005 to 2015. Atmos. Chem. Phys. 16, 4605–4629. https://doi.org/10.5194/acp-16-4605-2016

Kumar, P., Hama, S., Omidvarborna, H., Sharma, A., Sahani, J., Abhijith, K. V, Debele, S.E., Zavala-Reyes, J.C., Barwise, Y., Tiwari, A. (2020). Temporary reduction in fine particulate matter due to 'anthropogenic emissions switch-off' during COVID-19 lockdown in Indian cities. Sustain. Cities Soc. 62, 102382. https://doi.org/10.1016/j.scs.2020.102382

Kumar, R., Barth, M.C., Nair, V.S., Pfister, G.G., Suresh Babu, S., Satheesh, S.K., Krishna Moorthy, K., Carmichael, G.R., Lu, Z., Streets, D.G. (2015). Sources of black carbon aerosols in South Asia and surrounding regions during the Integrated Campaign for Aerosols, Gases and Radiation Budget (ICARB). Atmos. Chem. Phys. 15, 5415–5428. https://doi.org/10.5194/acp-15-5415-2015

Kurokawa, J., Ohara, T. (2019). Long-term historical trends in air pollutant emissions in Asia: Regional Emission inventory in ASia (REAS) version 3.1. Atmos. Chem. Phys. Discuss. 2019, 1–51. https://doi.org/10.5194/acp-2019-1122

Lai, C.C., Shih, T.P., Ko, W.C., Tang, H.J., Hsueh, P.R. (2020). Severe acute respiratory syndrome coronavirus 2 (SARS-CoV-2) and coronavirus disease-2019 (COVID-19): The epidemic and the challenges. Int. J. Antimicrob. Agents 55, 105924. https://doi.org/10.1016/j.ijantimicag.2020.105924

Landgraf, J., Aan De Brugh, J., Scheepmaker, R., Borsdorff, T., Hu, H., Houweling, S., Butz, A., Aben, I., Hasekamp, O. (2016). Carbon monoxide total column retrievals from TROPOMI shortwave infrared measurements. Atmos. Meas. Tech. 9, 4955–4975. https://doi.org/10.5194/amt-9-4955-2016

Lelieveld, J., Evans, J.S., Fnais, M., Giannadaki, D., Pozzer, A. (2015). The contribution of outdoor air pollution sources to premature mortality on a global scale. Nature 525, 367–371. https://doi.org/10.1038/nature15371

Lelieveld, J., Klingmüller, K., Pozzer, A., Burnett, R.T., Haines, A., Ramanathan, V. (2019). Effects of fossil fuel and total anthropogenic emission removal on public health and climate. PNAS 116, 7192–7197. https://doi.org/10.1073/pnas.1819989116

Levelt, P.F., Hilsenrath, E., Leppelmeier, G.W., van den Oord, G.H.J., Bhartia, P.K., Tamminen, J., de Haan, J.F., Veefkind, J.P. (2006). Science objectives of the ozone monitoring instrument. IEEE Trans. Geosci. Remote Sens. 44, 1199–1208. https://doi.org/10.1109/TGRS.2006.872336

Li, Q., Guan, X., Wu, P., Wang, X., Zhou, L., Tong, Y., Ren, R., Leung, K.S.M., Lau, E.H.Y., Wong, J.Y., Xing, X., Xiang, N., Wu, Y., Li, C., Chen, Q., Li, D., Liu, T., Zhao, J., Liu, M., Tu, W., *et al.* (2020). Early Transmission Dynamics in Wuhan, China, of Novel Coronavirus–Infected Pneumonia. N. Engl. J. Med. 382, 1199–1207. https://doi.org/10.1056/NEJMoa2001316

Madineni, V.R., Dasari, H.P., Karumuri, R., Viswanadhapalli, Y., Perumal, P., Hoteit, I. (2021). Natural processes dominate the pollution levels during COVID-19 lockdown over India. Sci. Rep. 11, 15110. https://doi.org/10.1038/s41598-021-94373-4

Mahapatra, P.S., Jain, S., Shrestha, S., Senapati, S., Puppala, S.P. (2018). Ambient endotoxin in PM_{10} and association with inflammatory activity, air pollutants, and meteorology, in Chitwan, Nepal. Sci. Total Environ. 618, 1331–1342. https://doi.org/10.1016/j.scitotenv.2017.09.249

Mahato, S., Pal, S., Ghosh, K.G. (2020). Effect of lockdown amid COVID-19 pandemic on air quality of the megacity Delhi, India. Sci. Total Environ. 730, 139086. https://doi.org/10.1016/j.scitotenv.2020.139086

Mangla, R., Indu, J., Chakra, S.S. (2020). Inter-comparison of multi-satellites and Aeronet AOD over Indian Region. Atmos. Res. 240, 104950. https://doi.org/10.1016/j.atmosres.2020.104950

Martin, R.V. (2008). Satellite remote sensing of surface air quality. Atmos. Environ. 42, 7823–7843. https://doi.org/10.1016/j.atmosenv.2008.07.018

Martin, R.V., Brauer, M., van Donkelaar, A., Shaddick, G., Narain, U., Dey, S. (2019). No one knows which city has the highest concentration of fine particulate matter. Atmos. Environ. X 3, 100040. https://doi.org/10.1016/j.aeaoa.2019.100040

McNeill, V.F. (2020). COVID-19 and the air we breathe. ACS Earth Space Chem. 4, 674–675. https://doi.org/10.1021/acsearthspacechem.0c00093

Mehra, M., Panday, A.K., Puppala, S.P., Sapkota, V., Adhikary, B., Pokheral, C.P., Ram, K. (2019). Impact of local and regional emission sources on air quality in foothills of the Himalaya during spring 2016: An observation, satellite and modeling perspective. Atmos. Environ. 216, 116897. https://doi.org/10.1016/j.atmosenv.2019.116897

Menut, L., Bessagnet, B., Siour, G., Mailler, S., Pennel, R., Cholakian, A. (2020). Impact of lockdown measures to combat Covid-19 on air quality over western Europe. Sci. Total Environ. 741, 140426. https://doi.org/10.1016/j.scitotenv.2020.140426

Metya, A., Dagupta, P., Halder, S., Chakraborty, S., Tiwari, Y.K. (2020). COVID-19 lockdowns improve air quality in the South-East Asian regions, as seen by the remote sensing satellites. Aerosol Air Qual. Res. 20, 1772–1782. https://doi.org/10.4209/aaqr.2020.05.0240

Nakada, L.Y.K., Urban, R.C. (2020). COVID-19 pandemic: Impacts on the air quality during the partial lockdown in São Paulo state, Brazil. Sci. Total Environ. 730, 139087. https://doi.org/10.1016/j.scitotenv.2020.139087

Pandey, S.K., Vinoj, V. (2021). Surprising Changes in aerosol loading over India amid COVID-19 lockdown. Aerosol Air Qual. Res. 21, 200466. https://doi.org/10.4209/aaqr.2020.07.0466

Pathakoti, M., Muppalla, A., Hazra, S., Dangeti, M., Shekhar, R., Jella, S., Mullapudi, S.S., Andugulapati, P., Vijayasundaram, U. (2020). An assessment of the impact of a nation-wide lockdown on air pollution – a remote sensing perspective over India (preprint). Atmos. Chem. Phys. Discuss. [preprint], https://doi.org/10.5194/acp-2020-621

Philip, S., Martin, R. V, Snider, G., Weagle, C.L., van Donkelaar, A., Brauer, M., Henze, D.K., Klimont, Z., Venkataraman, C., Guttikunda, S.K., Zhang, Q. (2017). Anthropogenic fugitive, combustion and industrial dust is a significant, underrepresented fine particulate matter source in global atmospheric models. Environ. Res. Lett. 12, 44018. https://doi.org/10.1088/1748-9326/aa65a4

Phua, J., Weng, L., Ling, L., Egi, M., Lim, C.M., Divatia, J.V., Shrestha, B.R., Arabi, Y.M., Ng, J., Gomersall, C.D., Nishimura, M., Koh, Y., Du, B. (2020). Intensive care management of coronavirus disease 2019 (COVID-19): Challenges and recommendations. Lancet Respir. Med. 8, 506–517. https://doi.org/10.1016/S2213-2600(20)30161-2

Purohit, P., Amann, M., Kiesewetter, G., Rafaj, P., Chaturvedi, V., Dholakia, H.H., Koti, P.N., Klimont, Z., Borken-Kleefeld, J., Gomez-Sanabria, A., Schöpp, W., Sander, R. (2019). Mitigation pathways towards national ambient air quality standards in India. Environ. Int. 133, 105147. https://doi.org/10.1016/j.envint.2019.105147

Putero, D., Cristofanelli, P., Marinoni, A., Adhikary, B., Duchi, R., Shrestha, S.D., Verza, G.P., Landi, T.C., Calzolari, F., Busetto, M., Agrillo, G., Biancofiore, F., Di Carlo, P., Panday, A.K., Rupakheti, M., Bonasoni, P. (2015). Seasonal variation of ozone and black carbon observed at Paknajol, an urban site in the Kathmandu Valley, Nepal. Atmos. Chem. Phys. 15, 13957–13971. https://doi.org/10.5194/acp-15-13957-2015

Rai, M., Mahapatra, P.S., Gul, C., Kayastha, R.B., Panday, A.K., Puppala, S.P. (2019). Aerosol radiative forcing estimation over a remote high-altitude location (4900 masl) near Yala Glacier, Nepal. Aerosol Air Qual. Res. 19, 1872–1891. https://doi.org/10.4209/aaqr.2018.09.0342

Ranjan, A.K., Patra, A.K., Gorai, A.K. (2020). Effect of lockdown due to SARS COVID-19 on aerosol optical depth (AOD) over urban and mining regions in India. Sci. Total Environ. 745, 141024.

https://doi.org/10.1016/j.scitotenv.2020.141024

Rupakheti, D., Adhikary, B., Praveen, P.S., Rupakheti, M., Kang, S., Mahata, K.S., Naja, M., Zhang, Q., Panday, A.K., Lawrence, M.G. (2017). Pre-monsoon air quality over Lumbini, a world heritage site along the Himalayan foothills. Atmos. Chem. Phys. 17, 11041–11063. https://doi.org/10.5194/acp-17-11041-2017

Sadavarte, P., Venkataraman, C., Cherian, R., Patil, N., Madhavan, B.L., Gupta, T., Kulkarni, S., Carmichael, G.R., Adhikary, B. (2016). Seasonal differences in aerosol abundance and radiative forcing in months of contrasting emissions and rainfall over northern South Asia. Atmos. Environ. 125, 512–523. https://doi.org/10.1016/j.atmosenv.2015.10.092

Saikawa, E., Panday, A., Kang, S., Gautam, R., Zusman, E., Cong, Z., Somanathan, E., Adhikary, B. (2019). Air Pollution in the Hindu Kush Himalaya, in: Wester, P., Mishra, A., Mukherji, A., Shrestha, A.B. (Eds.), The Hindu Kush Himalaya Assessment, Springer International Publishing, Cham, pp. 339–387. https://doi.org/10.1007/978-3-319-92288-1_10

Shakoor, A., Chen, X., Farooq, T.H., Shahzad, U., Ashraf, F., Rehman, A., Sahar, N. e., Yan, W. (2020). Fluctuations in environmental pollutants and air quality during the lockdown in the USA and China: Two sides of COVID-19 pandemic. Air Qual. Atmos. Health 13, 1335–1342. https://doi.org/10.1007/s11869-020-00888-6

Sharma, R., Bhattarai, S., Rupakheti, M. (2020a). Lockdown caused by COVID-19 pandemic reduces air pollution in cities worldwide. Preprint 1–25. https://doi.org/10.31223/osf.io/edt4j

Sharma, S., Zhang, M., Anshika, Gao, J., Zhang, H., Kota, S.H. (2020b). Effect of restricted emissions during COVID-19 on air quality in India. Sci. Total Environ. 728, 138878. https://doi.org/10.1016/j.scitotenv.2020.138878

Shrestha, R.M. (2018). Emissions of air pollutants and greenhouse gases in Nepal. Regional Energy Resources Information Center (RERIC), Asian Institute of Technology, Thailand. http://www.rrcap.ait.ac.th/Publications/emissionGreenhouseGasNepal.pdf

Silva, R.A., Adelman, Z., Fry, M.M., West, J.J. (2016). The impact of individual anthropogenic emissions sectors on the global burden of human mortality due to ambient air pollution. Environ. Health Perspect. 124, 1776–1784. https://doi.org/10.1289/EHP177

Stone, E.A., Schauer, J.J., Pradhan, B.B., Dangol, P.M., Habib, G., Venkataraman, C., Ramanathan, V. (2010). Characterization of emissions from South Asian biofuels and application to source apportionment of carbonaceous aerosol in the Himalayas. J. Geophys. Res. 115, D06301. https://doi.org/10.1029/2009JD011881

United Nations (2019). World Population Prospects 2019. Department of Economic and Social Affairs, United Nations. https://population.un.org/wpp/

Upadhyay, A., Dey, S., Chowdhury, S., Goyal, P. (2018). Expected health benefits from mitigation of emissions from major anthropogenic $PM_{2.5}$ sources in India: Statistics at state level. Environ. Pollut. 242, 1817–1826. https://doi.org/10.1016/j.envpol.2018.07.085

Vadrevu, K.P., Lasko, K., Giglio, L., Schroeder, W., Biswas, S., Justice, C. (2019). Trends in Vegetation fires in South and Southeast Asian Countries. Sci. Rep. 9, 7422. https://doi.org/10.1038/s41598-019-43940-x

van der Werf, G.R., Randerson, J.T., Giglio, L., van Leeuwen, T.T., Chen, Y., Rogers, B.M., Mu, M., van Marle, M.J.E., Morton, D.C., Collatz, G.J., Yokelson, R.J., Kasibhatla, P.S. (2017). Global fire emissions estimates during 1997--2016. Earth Syst. Sci. Data 9, 697–720. https://doi.org/10.5194/essd-9-697-2017

Veefkind, J.P., Aben, I., McMullan, K., Förster, H., de Vries, J., Otter, G., Claas, J., Eskes, H.J., de Haan, J.F., Kleipool, Q., van Weele, M., Hasekamp, O., Hoogeveen, R., Landgraf, J., Snel, R., Tol, P., Ingmann, P., Voors, R., Kruizinga, B., Vink, R., *et al.* (2012). TROPOMI on the ESA Sentinel-5 Precursor: A GMES mission for global observations of the atmospheric composition for climate, air quality and ozone layer applications. Remote Sens. Environ. 120, 70–83. https://doi.org/10.1016/j.rse.2011.09.027

Venter, Z.S., Aunan, K., Chowdhury, S., Lelieveld, J. (2020). COVID-19 lockdowns cause global air pollution declines with implications for public health risk (preprint). Epidemiology https://doi.org/10.1101/2020.04.10.20060673

Wang, P., Chen, K., Zhu, S., Wang, P., Zhang, H. (2020). Severe air pollution events not avoided by reduced anthropogenic activities during COVID-19 outbreak. Resour. Conserv. Recycl. 158, 104814. https://doi.org/10.1016/j.resconrec.2020.104814

Wei, J., Li, Z., Peng, Y., Sun, L. (2019a). MODIS Collection 6.1 aerosol optical depth products over land and ocean: validation and comparison. Atmos. Environ. 201, 428–440. https://doi.org/10.1016/j.atmosenv.2018.12.004

Wei, J., Peng, Y., Guo, J., Sun, L. (2019b). Performance of MODIS Collection 6.1 Level 3 aerosol products in spatial-temporal variations over land. Atmos. Environ. 206, 30–44. https://doi.org/10.1016/j.atmosenv.2019.03.001

Wester, P., Mishra, A., Mukherji, A., Shrestha, A.B. (2019). The Hindu Kush Himalaya Assessment: Mountains, Climate Change, Sustainability and People. Springer International Publishing, Cham. https://doi.org/10.1007/978-3-319-92288-1

WHO Newsroom (2020). WHO Timeline - COVID-19. World Health Organization.

World Bank (2020). Global Economic Prospects, June 2020. World Bank, Washington, DC. https://doi.org/10.1596/978-1-4648-1553-9

World Health Organization (WHO) (2022). Ambient air pollution data. https://www.who.int/data/gho/data/themes/air-pollution/ambient-air-pollution

Yadav, R., Sahu, L.K., Beig, G., Tripathi, N., Jaaffrey, S.N.A. (2017). Ambient particulate matter and carbon monoxide at an urban site of India: Influence of anthropogenic emissions and dust storms. Environ. Pollut. 225, 291–303. https://doi.org/10.1016/j.envpol.2017.01.038

Zambrano-Monserrate, M.A., Ruano, M.A., Sanchez-Alcalde, L. (2020). Indirect effects of COVID-19 on the environment. Sci. Total Environ. 728, 138813. https://doi.org/10.1016/j.scitotenv.2020.138813

Zhang, M., Katiyar, A., Zhu, S., Shen, J., Xia, M., Ma, J., Kota, S.H., Wang, P., Zhang, H. (2021). Impact of reduced anthropogenic emissions during COVID-19 on air quality in India. Atmos. Chem. Phys. 21, 4025–4037. https://doi.org/10.5194/acp-21-4025-2021